Date of Publication: 11th May 2026
ISSN: 2737-713X

SATELLITE-BASED ASSESSMENT OF COASTAL DEFENCE EFFECTIVENESS AND SHORELINE DYNAMICS ALONG THE DZITA COAST, GHANA (2001-2023)

*[1]John David K.T. Kudadjie, [1]Elikplim A. Dzikunoo, [1]Yvonne S.A. Loh, [2]Fon A. Zoum

[1] *Department of Earth Science, University of Ghana; P.O. Box LG 25 Legon, Ghana*
[2] *Department of Mining and Mineral Engineering, National Higher Polytechnic Institute, University of Bamenda; P.O. Box 39, Cameroon*
***Corresponding author:** jdkudadjie@outlook.com*

Abstract

Coastal erosion, driven by wave action, sea-level rise, and severe weather events threatens communities and infrastructure globally, yet effectiveness of coastal defence structures under climate change remains inadequately evaluated. This study quantified shoreline change rates along Ghana's Dzita coast and assessed the impact of Atorkor-Dzita-Anyanui sea defence project over two decades (2001-2023), while exploring relationships between shoreline dynamics and climate-induced sea-level rise. Shoreline positions were extracted from LANDSAT 7 imagery using modified normalized difference water index (MNDWI) and sub-pixel contour mapping for pre-defence (2001-2014) and post-defence (2014-2023) periods. Annual growth/retreat values were compared against the 2023 baseline and correlated with global mean sea-level data using Spearman rank correlation. Pre-defence erosion averaged -4.0 $\pm$ 1.4 m/year indicating substantial retreat. Post-defence showed a net accretion averaging +1.7 $\pm$ 1.7 m/year, representing an improvement and demonstrating effective erosion mitigation. As documented in existing literature, the broader Keta Sea defence system has exacerbated downdrift erosion at Kedzi and Hlorve. Correlation analysis between shoreline changes and sea-level rise yielded inconclusive results (p-value = 0.5774), indicating a quasi-linear relationship influenced by complex interactions including human activities, sediment dynamics, and coastal infrastructure beyond sea-level rise alone. These findings demonstrate successful local-scale coastal protection while underscoring the need for comprehensive, adaptive coastal management strategies that account for both protective benefits and unintended downdrift impacts, providing data-driven insights for policymakers addressing climate adaptation challenges along sediment-starved coastlines.

Keywords
coastal erosion, sea-level rise, coastal defence effectiveness, satellite remote sensing, Digital Earth Africa

Introduction

The last decade (2010-2020) was the warmest on record for both land and ocean, with each successive decade since the 1990s being warmer. Greenland and Antarctica lost 38% more ice between 2011 and 2020 than between 2001 and 2010 World Meteorological Organization (2020). Exacerbated by climate change, intensifying storms and rising sea levels escalate coastal erosion by producing stronger winds, larger waves, and more frequent inundation events, collectively leading to increased coastal erosion rates and destruction of critical coastal infrastructure. In Ghana, the Keta region has experienced significant shoreline loss due to coastal erosion throughout the 20th century (Appeaning Addo et al., 2011; Boateng, 2012; Ly, 1980). By 1996, over half of Keta and its neighboring rural areas had been lost to erosion and flooding, affecting more than 10,000 people and causing substantial economic harm (Danquah et al., 2014; Ile et al., 2014; Oteng-Ababio and Owusu, 2011). The Keta Sea Defence project was initiated to address the alarming erosion rate of 4-8 meters per year (Ly, 1980), successfully reducing it to approximately 2 m per year post-construction (Jayson-Quashigah et al., 2013). However, the project also caused increased down-drift erosion in some locations, with rates increasing to 8 m per year in certain areas (Adu-Gyamfi et al., 2020).

Satellite-based shoreline monitoring has emerged as a cost-effective alternative to traditional field-based methods for erosion monitoring. The Modified Normalized Difference Water Index (MNDWI) effectively delineates land-water boundaries by exploiting the spectral contrast between green and shortwave infrared bands (Xu, 2006). Combined with sub-pixel contour mapping techniques, MNDWI-based approaches achieve shoreline detection accuracy beyond nominal satellite spatial resolution (Bishop-Taylor et al., 2019). The integration of tidal modeling, particularly using the FES2014 global tide model (Carrere et al., 2016), enables the extraction of shorelines from consistent tidal datums, minimizing uncertainty from tidal variations. Bishop-Taylor et al. (2021b) developed a comprehensive framework combining these methods to map Australia's coastline using Landsat imagery, which was subsequently adapted for Africa using Digital Earth Africa's freely accessible coastline products (Krause et al., 2021).

The emergence of Digital Earth Africa coastline products (as adapted from Digital Earth Australia (DEA)) present new opportunities for coastal monitoring in Ghana. While valuable research has documented shoreline changes along Ghana's coast (Appeaning Addo et al., 2011; Boateng, 2012; Jayson-Quashigah et al., 2013), the recent availability of freely accessible, analysis-ready Landsat archives and automated extraction tools now enables systematic annual monitoring over multiple decades with consistent methodology. Despite these capabilities, systematic application of Digital Earth Africa tools for multi-decadal assessment of coastal defence perfor-

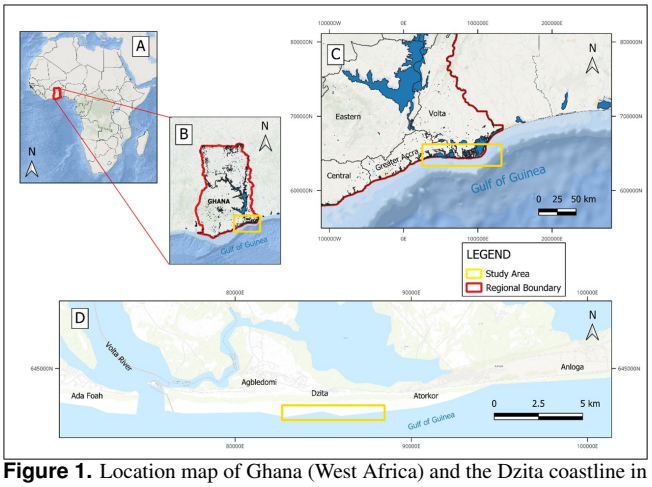

Figure 1. Location map of Ghana (West Africa) and the Dzita coastline in southeastern Ghana

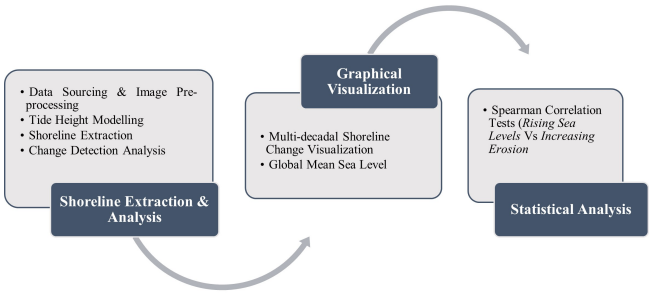

Figure 2. Methodological workflow for assessing shoreline dynamics along the Dzita coast, southeast of Ghana. This three-stage methodology combines remote sensing analysis, visualization, and statistical testing to assess shoreline response to the Atorkor-Dzita-Anyanui sea defence project and evaluate correlations with global sea-level rise

mance in Ghana has not been extensively undertaken. This study addresses this gap by utilizing Digital Earth Africa's Landsat imagery services and open-source shoreline analysis tools to quantify shoreline change rates along the Dzita coast over two decades (2001-2023), comparing pre and post-defence periods to systematically assess coastal defence effectiveness while statistically examining correlations between shoreline dynamics and climate-induced sea-level rise.

Study Area

Ghana's coastline can be broken down into the western, central, and eastern (Ly, 1980) coasts, with the coast under study falling within the eastern coast and covering approximately 2 km of this stretch, from the eastern outskirts of the Agbledomi to the outskirts west of Atorkor as shown in Figure 1.

This shoreline generally falls within the Keta Municipality. Keta's distinctive terrain features a vast, shallow lagoon known as the Keta Lagoon complex, encircled by marshlands. A slender sandbar, measuring just over 2.5 km at its widest point and rising up to 2 m above sea level, separates the lagoon from the Gulf of Guinea, while several creeks line the coastline (Awadzi et al., 2008; Boateng, 2009). According to Akpati (1978), the geology of the area is characterized by soft quaternary rocks and unconsolidated sediments composed of clay, loose sand, and gravel deposits rendering it particularly susceptible to coastal erosion. These materials lack the strength to withstand the abrasive forces of waves and currents. Clay particles are fine-grained and easily dislodged, whereas loose sand beaches and gravel are readily transported by water movement, leading to progressive loss of the shoreline. Keta is heavily influenced by fluvial sediments deposited by the Volta River as well as marine and fluvial-marine sediments and has two types of waves: locally generated seas from the weak monsoon and swells from storms in the southern Atlantic Ocean. The tides in the area are semi-diurnal, with an average range of approximately 1 m, and tidal currents are generally weak (Appeaning Addo et al., 2011). Scientific consensus indicates that climate change is a significant driver of rising sea levels, which in turn intensifies coastal erosion (IPCC, 2023). As global temperatures rise, glaciers and polar ice caps melt, contributing to higher sea levels that increase the frequency and intensity of coastal flooding and erosion. Regions with a long history of coastal erosion, such as Keta, are particularly vulnerable to these changes. However, coastal erosion does not happen in isolation. Human activities, such as sand mining and urban development, have significantly contributed to the erosion in Keta. The loss of property and infrastructure due to coastal erosion has profound socioeconomic implications for local communities, including displacement, loss of livelihood, and increased poverty. Over the years, several defence projects have been initiated, including the construction of sea walls and groynes, aimed at mitigating erosion and protecting local communities (Adu-Gyamfi et al., 2020).

Materials and Methods

The methodology demonstrated in this study as seen in Figure 2 is an adaptation of Bishop-Taylor et al. (2021b). All analyses were conducted using Python 3.10.x with the following key packages: Open Data Cube (datacube v1.9.x), Xarray (Hoyer and Hamman, 2017), DEA Tools (Krause et al., 2021), DEA Coastlines (Bishop-Taylor et al., 2021a), eo-tides for tidal modeling, geopandas for vector processing, and rioxarray for geospatial raster operations. The complete computational environment and package versions are documented in the Jupyter notebook provided as Supplementary Data S1.

A detailed technical methodology workflow (Jupyter notebook) can be found at `https://github.com/Kudadjie/dzita_coastal_erosion_studies` as adapted from the DE Africa jupyter notebook example on coastal erosion analysis. The complete computational workflow including all Python code, parameters, and processing steps is also provided in Supplementary Data S1 (SDS1).

Data Sourcing and Image Pre-processing

Landsat 7 imagery (30 m spatial resolution) was selected from the Digital Earth Africa datacube based on data availability and temporal consistency across the pre-defence (2001-2013)

and post-defence (2014-2023) periods. The analysis utilized USGS Landsat Collection 2 Level 2 surface reflectance products, which are preprocessed to Analysis-Ready Data (ARD) standards including geometric correction, radiometric calibration, and atmospheric correction using the LEDAPS (Landsat Ecosystem Disturbance Adaptive Processing System) algorithm (Masek et al., 2006; USGS, 2020). Bands 1 (blue), 2 (green), 3 (red), and 5 (shortwave infrared) were used for shoreline extraction. Cloud masking was applied automatically using Digital Earth Africa's pixel quality assessment algorithms, which filter observations based on cloud probability and quality flags. All imagery was reprojected to the WGS84 geographic coordinate system (EPSG:4326) for consistency with global datasets.

Tide height modeling

Satellite imagery acquired from the datacube included images captured at different tide levels, hence it was essential to filter those captured at undesirable tide heights (high tide or low tide). Tidal heights were computed at each pixel location using the eo-tides Python package (Bishop-Taylor et al., 2021b) with the FES2014 global tidal model, which provides tidal predictions with a root mean square accuracy of approximately 4 cm in deep ocean regions (Carrere et al., 2016). Images were filtered to retain only those captured within 50% of the observed tidal range centered at mean sea level (tide_centre = 0.0 m), following the methodology of Bishop-Taylor et al. (2021b). This adaptive tidal filtering approach accounts for local tidal variability ($\sim$1 m range in the study area) while ensuring consistent water level conditions across all analyzed imagery, effectively constraining observations to mid-tide conditions.

Shoreline Extraction

Differentiating land from water

To extract shoreline positions, it is necessary to distinguish land from water. Using Python computation based on the Modified Normalized Difference Water Index (MNDWI) (Xu, 2006), as shown in Figure 3, the presence of water was identified by calculating the ratio between the green and shortwave-infrared (SWIR) radiation using Landsat's green and SWIR 1 bands:

$$\text{Modified Normalized Difference Water Index (MNDWI)} = \frac{\text{Green} - \text{SWIR 1}}{\text{Green} + \text{SWIR 1}} \quad (1)$$

A fixed MNDWI threshold value of 0 was applied to classify pixels as water (MNDWI > 0) or land (MNDWI $\leq$ 0), following the approach demonstrated in Bishop-Taylor et al. (2021b) for coastal applications. This threshold capitalizes on the fundamental spectral properties of water bodies, which exhibit positive MNDWI values due to higher reflectance in the green band compared to shortwave infrared. A typical MNDWI map of the area under study can be seen in Figure 3.

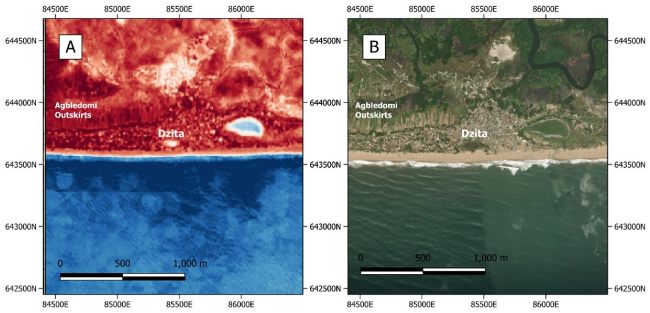

Figure 3. (A) MNDWI map of coastline along Dzita coast showing the clear distinction between water (shades of blue) and land (shades of red) timestamped at 2019

Annual composites

Remote sensing images often contain noise, such as clouds or cloud shadows in optical images and wind effects on water in radar images. Composite or *summary* images were created by merging multiple images into one to generate clearer imagery that allows for easier comparison over time. These composites captured the median or *typical* view of the study area during a specific time frame, and the median was chosen to avoid distortion of the data by extreme outliers.

Extraction of shorelines

Using the open-source *sub-pixel contours* mapping method (Bishop-Taylor et al., 2019; Krause et al., 2021) on the 30 m resolution tidally-masked annual MNDWI composites, precise shoreline contours for each annual composite were drawn to delineate the boundary between land and water. Contours were extracted using the sub-pixel contours algorithm implemented in the DEA Tools Python package (Krause et al., 2021), which applies Marching Squares edge detection with linear interpolation to achieve shoreline positioning accuracy beyond the nominal 30 m Landsat pixel resolution (Bishop-Taylor et al., 2019). Contours with fewer than 15 vertices were excluded to remove spurious detections and ensure only continuous shoreline features were retained.

Change Detection Analysis

To detect areas of the coastline that were undergoing rapid change, a computational method was employed where evenly spaced points were generated every 20 m along the most recent shoreline (2023) to serve as reference points. The distances from these reference points to each annual shoreline were calculated. Negative distances indicate that the annual shoreline was positioned inland relative to the reference points, whereas positive distances signified that the shoreline had shifted seaward. As the reference points are based on the most recent shoreline, the distance for that year will always be zero. The rate of change (R) for each reference point was calculated by linearly regressing the annual shoreline cross-shore distance with respect to time:

$$R = \frac{\sum_{i=1}^{n}(t_i - \bar{t})(d_i - \bar{d})}{\sum_{i=1}^{n}(t_i - \bar{t})^2} \quad (2)$$

where R is the annual rate of coastal change (in meters per year), t_i is the year of observation, d_i is the cross-shore distance of the shoreline from the reference point (baseline year) for year i, $\bar{t}$ is the mean of all observation years, $\bar{d}$ is the mean of all distances, and n is the number of annual observations. Negative values of R indicate coastal retreat (erosion), whereas positive values indicate coastal growth (accretion or progradation). Computation was done in the Jupyter notebook containing the technical methodology (Supplementary Data S1). The rates of change calculated for each point were compared to the baseline year. The complete shoreline change rate data for all reference points and years are provided in Supplementary Data S2, and the extracted annual shoreline position data are provided in Supplementary Data S3.

Pre/Post-Defence Rate of Shoreline Change

To quantitatively assess the effectiveness of the Atorkor-Dzita-Anyanui sea defence project, shoreline change rates were calculated separately for pre-defence (2001-2014) and post-defence (2014-2023) periods. For each of the reference points along the study coastline, period-specific erosion rates were computed using the annual cross-shore distance measurements from the change detection analysis. The pre-defence erosion rate (R_{pre}) for each point was calculated as:

$$R_{pre} = \frac{D_{2014} - D_{2001}}{13} \tag{3}$$

where D_{2014} and D_{2001} represent the cross-shore distances of the shoreline from the reference point (2023 baseline) in years 2014 and 2001 respectively, and 13 represents the number of years in the pre-defence period. Similarly, the post-defence rate (R_{post}) was calculated as:

$$R_{post} = \frac{D_{2023} - D_{2014}}{9} \tag{4}$$

where D_{2023} and D_{2014} represent the cross-shore distances in years 2023 and 2014 respectively, and 9 represents the number of years in the post-defence period. The year 2014 was selected as the transition point based on the completion date of major seawall construction in the study area.

For each period, summary statistics were calculated across all reference points including mean rate, standard deviation, minimum and maximum rates, and the proportion of points exhibiting erosional (negative) versus accretional (positive) trends. Negative rate values indicate landward shoreline retreat (erosion), while positive values indicate seaward shoreline advance (accretion). The change in erosion rate between periods was assessed by comparing mean pre-defence and post-defence rates. All calculations were performed using Python 3.10 and exported to spreadsheet format for verification (Supplementary Data S2).

Shoreline Change Visualization

Point distances generated for each year were then visualized using stacked area plots, where the values were cumulatively summed to illustrate progressive shoreline movement patterns over time. This cumulative representation enabled the visualization of the total magnitude of the shoreline changes at each reference point across the study period.

Sea Level Data and Statistical Analysis

Global Mean Sea Level Data

To provide context for the relationship between sea levels and varying rates of coastal erosion and accretion during the study period, global mean sea level data from NASA's Sea Level Change Program (Beckley et al., 2017) was used as local sea-level data for the study area was unavailable. The dataset, spanning September 1992 to January 2024, accounted for global isostatic adjustment and excluded annual and semi-annual signals. As water level measurements were recorded multiple times per year, these readings were averaged to determine the representative annual mean for each year. The annual mean global sea level data used in this study are provided in Supplementary Data S4.

Statistical Tests

Spearman's rank correlation coefficient (ρ) was employed to explore whether long-term shoreline variability exhibits any monotonic relationship with global mean sea-level trends. This non-parametric test was selected because it does not assume a linear relationship between variables and is robust to outliers, making it appropriate for examining complex coastal dynamics where multiple interacting factors may influence shoreline position. The Spearman correlation coefficient was calculated as follows:

$$\rho = 1 - \frac{6\sum d_i^2}{n(n^2-1)} \tag{5}$$

where d_i is the difference between the ranks of the corresponding values of the two variables (shoreline change and sea level rise), and n is the number of data pairs. The coefficient ranges from -1 to +1, where values close to +1 indicate a strong positive correlation, values close to -1 indicate a strong negative correlation, and values near 0 indicate weak or no correlation. These tests paired individual data points representing erosion or accretion with the corresponding annual average GMSL values during the study period.

Limitations

Several limitations should be considered when interpreting the findings of this study. Landsat 7 imagery provides 30-meter spatial resolution, which limits detection of sub-pixel shoreline changes and small-scale coastal features. While sub-pixel contour extraction techniques enhance precision beyond the nominal pixel size (Bishop-Taylor et al., 2019), inherent uncertainty remains, particularly in areas with complex land-water boundaries, gradual beach slopes, or high suspended sediment concentrations that affect water index values. Annual shoreline positions represent median conditions over each year rather than capturing seasonal or storm-event variations. Short-term erosion or accretion episodes occurring between annual composites may not be fully represented in

the analysis.

Using global mean sea level rather than local tide gauge measurements introduces uncertainty. Regional sea-level variations can differ substantially from the global mean due to ocean dynamics, land subsidence, and gravitational effects from ice mass changes. While local sea-level monitoring stations exist in Ghana, continuous long-term records spanning the full 2001-2023 study period with consistent temporal coverage were not accessible for this analysis. GMSL data provide consistent global coverage and temporal continuity but do not capture regional variations in sea-level change.

This study infers sediment transport patterns from observed shoreline changes but does not directly measure sediment volumes, transport rates, or sources. Quantitative sediment budget analysis would require additional field measurements and hydrodynamic modeling. Attributing observed shoreline changes to specific drivers (coastal defence, sea-level rise, sediment supply) remains challenging given multiple interacting factors. While statistical analysis examines correlation with sea-level rise, causation cannot be definitively established from observational data alone. The study focuses on a specific 2-kilometer coastal segment over a 22-year period. Transferability of findings to other locations along Ghana's coast or longer time scales should be approached cautiously, recognizing site-specific conditions that may differ elsewhere.

Despite these limitations, the study provides valuable quantitative assessment of coastal defence effectiveness using freely available satellite data and open-source analysis tools, demonstrating a replicable monitoring methodology applicable to coastal management contexts where field-based monitoring resources are limited.

Results and Dsicussion

Results

Shoreline change dynamics: pre- and post-sea defence periods

A comparative analysis of shoreline patterns during the pre-sea defence (2001-2014, Figure 4b) and post-sea defence (2015-2023, Figure 4c) periods revealed significant shifts in coastal dynamics. Prior to the seawall construction, the coastline experienced substantial erosion, evidenced by the pronounced retreat of the shoreline. The spatial pattern of shoreline change shows clear demarcation between defended and undefended segments. Protected areas exhibit net accretion or stability.

Rates of Shoreline Change: pre- and post-sea defence periods

Quantitative analysis of the generated reference points across the coast under study reveals a dramatic transformation in shoreline dynamics between the pre-defence and post-defence periods (Table 1).

During the pre-defence period (2001-2014), the entire study coastline experienced erosion, with mean retreat rates of -4.0 $\pm$ 1.4 m/year. Individual reference points showed erosion rates ranging from -7.4 m/year at the most severely affected locations to -1.6 m/year at the least affected areas. Following construction of the Atorkor-Dzita-Anyanui sea defence, the post-defence period (2014-2023) showed a complete reversal of this pattern. The mean shoreline change rate shifted to +1.7 $\pm$ 1.7 m/year, representing net accretion rather than erosion. The high standard deviation (1.7 m/year, equal to the mean rate) reflects considerable spatial variability in the post-defence response along the coastline, with some reference points continuing to experience modest erosion (down to -1.7 m/year) while others recorded substantial accretion (up to +4.8 m/year). This variability likely reflects differences in local wave exposure, proximity to defence structures, and sediment redistribution patterns along the protected reach. The range of individual point rates expanded from -1.7 to +4.8 m/year.

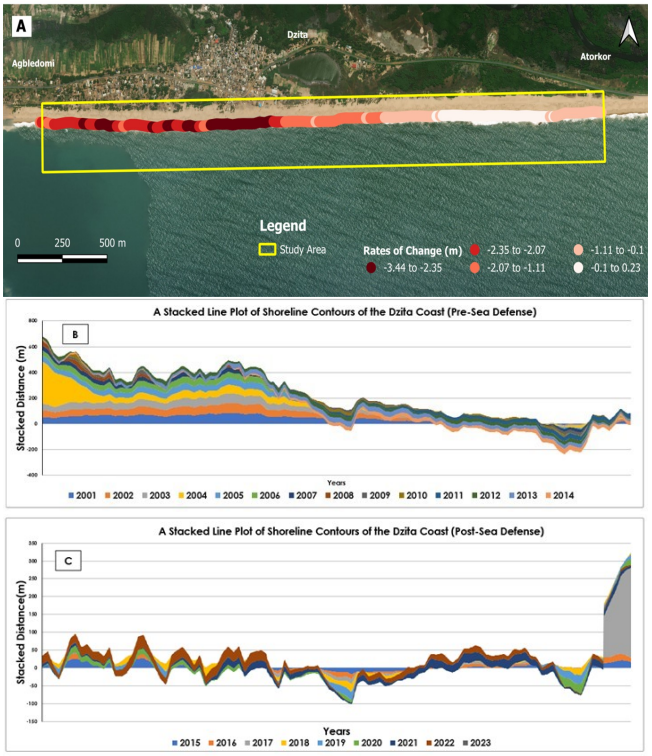

Figure 4. (A) Rates of Shoreline Change (Over entire time period; 2001-2023) along Dzita coast. Darker hues indicate higher rates of erosion whereas lighter hues indicate lower rates of erosion. Background imagery: Landsat 7 Collection-2 Level-2 (USGS). Projection: WGS 84 / UTM Zone 31N

Table 1. Summary of Shoreline Change Rates at Dzita Coast

Period	Duration (years)	Mean Rate (m/year)	Std Dev (m/year)	Range (m/year)
Pre-defence (2001–2014)	13	-4.0	1.4	-7.4 – -1.6
Post-defence (2014–2023)	9	+1.7	1.7	-1.7 – +4.8

Note: Negative values indicate erosion (landward retreat); positive values indicate accretion (seaward advance).

Table 2. Comparison of Shoreline Change Rates along Ghana's Eastern Coast

Location	Study Period	Mean Rate (m/year)	Range (m/year)	Conditions	Source
Keta Region	1974–1980	-6.0	-4 to -8	Pre-defence	Ly (1980)
Keta	1992–2010	-3.0	-2 to -4	Post-initial defence	Jayson-Quashigah et al. (2013)
Keta Beach	Post-2000s	-2.0	–	Post-groyne installation	Appeaning Addo et al. (2011)
Kedzi/Hlorve	Post-2000s	-8.0	–	Downdrift erosion	Adu-Gyamfi et al. (2020)
Dzita	2001–2014	-4.0 $\pm$ 1.4	-7.4 to -1.6	Pre-defence	This study
Dzita	2014–2023	+1.7 $\pm$ 1.7	-1.7 to +4.8	Post-defence	This study

Note: Negative values indicate erosion (landward retreat); positive values indicate accretion (seaward advance).

Figure 5. Satellite imagery of the Keta Municipal and its environs showing the study area; Dzita (labeled 'A') and the Kedzi/Hlorve areas (labeled 'B'). Imagery retrieved from Google Earth

Discussion

Quantitative Assessment of Sea Defence Effectiveness

The observed post-defence shoreline changes represent a substantial reduction in erosion rates compared to historical trends along Ghana's eastern coast. Table 2 presents a quantitative comparison of erosion rates from this study with previously published data for the broader Keta region.

Pre-defence erosion rates at Dzita (-4.0 $\pm$ 1.4 m/year, 2001-2014) align with the lower to middle range of historical Keta region rates documented by Ly (1980) prior to any coastal protection (-4 to -8 m/year). This suggests the Dzita coast experienced moderate erosion relative to the most severely affected areas of the broader Keta system. The pre-defence rates are also comparable to post-initial-defence conditions reported by Jayson-Quashigah et al. (2013) for the Keta area (-2 to -4 m/year), indicating that without local protection, the Dzita segment continued eroding at rates similar to other defended portions of the coastline. Post-defence, the reversal to net accretion (+0.5 to +3 m/year in protected areas) represents a significant shift, demonstrating effective erosion mitigation by the seawall structures. This performance is comparable to other protected segments along the Keta coastline documented by Jayson-Quashigah et al. (2013) and Angnuureng et al. (2023).

However, this local success must be viewed within the regional sediment transport context. Consistent with findings from Adu-Gyamfi et al. (2020), the broader Keta sea defence system has generated severe downdrift erosion at Kedzi and Hlorve (locations as seen in Figure 5), with rates reaching -8 m/year exceeding the pre-defence erosion rates at Dzita. This demonstrates that structural interventions that successfully stabilize one segment can intensify erosion elsewhere through disrupted longshore sediment transport.

Factors Controlling Shoreline Dynamics in the Study Area

Shoreline position along the Dzita coast results from complex interactions among multiple natural and anthropogenic factors. While sea-level rise provides the broader climatic context, local-scale processes exert dominant control over observed shoreline behavior.

Coastal Defence Infrastructure

The Atorkor-Dzita-Anyanui sea defence project represents the most direct human intervention influencing shoreline dynamics in the study area. The seawall structures physically constrain landward erosion, effectively fixing the shoreline position at defended locations. However, coastal defence structures fundamentally alter longshore sediment transport processes. Hard structures such as seawalls, revetments, and groynes disrupt the natural alongshore movement of sediment driven by wave action and littoral currents. Installing perpendicular structures like groynes promotes sediment accumulation on the updrift side while starving downdrift areas of sediment supply. This mechanism explains the well-documented downdrift erosion at Kedzi and Hlorve following the Keta Sea defence installation (Adu-Gyamfi et al., 2020).

The phenomenon is well-established in coastal engineering literature. Rangel-Buitrago et al. (2018) and Balaji et al. (2017) documented that altered sediment transport dynamics lead to downdrift erosion and new erosion hotspots, with landward erosion and alongshore erosion downdrift being common at seawalls, breakwaters, and groynes. A systematic review by Nassar et al. (2018) revealed that while sea defence structures can address erosion at specific sites, they typically shift the erosion region further downdrift rather than eliminating the problem.

Sediment Supply and Volta River Influence

Sediment availability constitutes a critical control on shoreline dynamics along Ghana's eastern coast. The Volta River

historically supplied substantial sediment to the coastal system, nourishing beaches along the Keta-Ada coastline through longshore transport. However, the construction of the Akosombo Dam in 1965 and subsequent impoundment of Lake Volta drastically reduced sediment discharge to the coast (Boateng, 2012; Ly, 1980). This sediment starvation effect compounds the erosion problem along the Keta region. With reduced sediment input from the Volta River, the coastal system operates under a sediment deficit, making beaches more vulnerable to wave-driven erosion. The longshore transport system, which naturally redistributes sediment along the coast, now moves limited sediment volumes, reducing the capacity for natural beach recovery following storm events.

The interaction between sediment starvation and coastal defence structures creates particularly challenging conditions. Groynes and seawalls designed to trap sediment can only retain what is available in the longshore transport system. In a sediment-starved environment, these structures may successfully protect localized areas but exacerbate downdrift erosion by further limiting already constrained sediment supply to adjacent coastlines. While direct measurements of sediment flux are beyond the scope of this study, the observed patterns of localized accretion at protected sites and continued erosion at unprotected locations suggest sediment redistribution rather than net sediment gain. This interpretation aligns with the sediment budget deficit scenario described by Ly (1980) and subsequent researchers studying the Keta coast.

Tidal Regime and Wave Climate

The study area experiences semi-diurnal tides with an average range of approximately 1 meter (Appeaning Addo et al., 2011). While this relatively modest tidal range might suggest limited tidal influence on shoreline position, the twice-daily tidal cycle affects the elevation at which wave energy impacts the beach face. During high tide, waves reach higher on the beach profile, potentially eroding dune systems and upper beach sediments. During low tide, wave energy concentrates on lower beach elevations. The semi-diurnal tidal regime also influences sediment transport patterns. Tidal currents, though generally weak in the region (Appeaning Addo et al., 2011), contribute to alongshore sediment movement in concert with wave-driven processes. The interaction between tidal elevation changes and wave action creates a dynamic system where the active erosion zone migrates vertically throughout the tidal cycle.

Wave climate exerts dominant control over sediment transport and erosion along the Dzita coast. The area experiences two primary wave types: locally generated wind waves from monsoon conditions and larger swells originating from storms in the southern Atlantic Ocean (Appeaning Addo et al., 2011). These swells, particularly during high-energy events, deliver substantial wave energy to the coastline, driving both cross-shore and longshore sediment transport. The interaction between wave climate and coastal defence structures determines local shoreline behaviour. Seawalls reflect wave energy, which can enhance scour at the structure toe and alter sediment transport patterns. Groynes interrupt longshore transport, creating sediment accumulation on the updrift side and sediment deficits on the downdrift side. The net effect depends on the balance between incident wave energy, structure design, and available sediment supply.

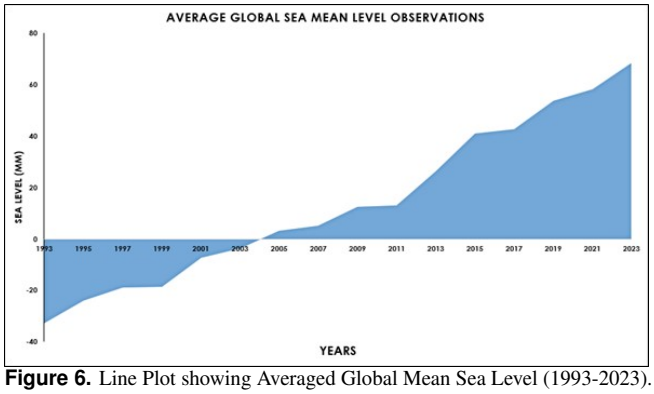

Figure 6. Line Plot showing Averaged Global Mean Sea Level (1993-2023). Data retrieved (2024-10-03) from GSFC (2021)

Human Activities Beyond Coastal Defence

Additional anthropogenic factors influence shoreline dynamics along Ghana's coast, though their specific impacts on the Dzita study area are not quantified in this analysis. Sand mining for construction materials, documented along various portions of Ghana's coastline, directly removes sediment from the coastal system, exacerbating erosion (Boateng, 2012). Urban development and vegetation removal reduce natural dune stability and eliminate the buffering capacity that dune systems provide against storm surge and wave attack. These cumulative human impacts create a complex management challenge where multiple stressors interact to influence shoreline position. Attributing observed changes to any single factor becomes problematic when coastal defence, sediment mining, river damming, and development pressures operate simultaneously.

Sea-Level Rise and Shoreline Correlation

Global mean sea level (GMSL) data from NASA reveals a consistent upward trend since 1993 (Figure 6), with an average rise of approximately 3.4 mm/year attributed to thermal expansion of seawater and melting of land-based ice (Beckley et al., 2017). This upward trend represents a significant climatic driver of coastal change, enhancing wave energy delivery to the coast, intensifying storm surge impacts, and increasing the frequency and duration of coastal inundation events.

Spearman's rank correlation analysis revealed no statistically significant monotonic relationship between annual shoreline change and global mean sea level (p-value = 0.5774 > 0.05), indicating that shoreline dynamics at Dzita are not directly coupled to global sea-level trends over the 22-year study period. While this finding may initially seem unexpected, it aligns with growing recognition in coastal science that the relationship between sea level rise and shoreline erosion is

complex and highly site-specific. Cazenave and Le Cozannet (2014) noted that while global mean sea level has been rising for several decades and a link between global coastal erosion and sea level rise has been suggested, conclusions from studies attempting to identify the specific role of sea level rise in shoreline changes remain controversial. Several studies show examples of rapid relative sea level changes leading to shoreline retreats, yet the high spatial variability of shoreline changes means that sea level rise impacts can only be evaluated at local scales. Research has shown that while sea level rise is associated with increased coastal erosion, the effects can be enhanced or counteracted by vertical land motion and morphological processes (Le Cozannet et al., 2015). The presence of the Keta Sea defence structures adds further complexity to the relationship between sea level rise and shoreline position in our study area. Coastal engineering structures fundamentally alter natural sediment transport processes and wave dynamics, potentially obscuring the direct effects of sea level rise on shoreline position. As noted in coastal vulnerability assessments, seven key parameters interact to define coastal environments: coastal feature, coastal elevation, coastal slope, coastline change rate, wave height, tidal range, and sea level rise (Pang et al., 2023). The interaction of these parameters, along with anthropogenic factors such as coastal protection structures, creates a comprehensive situation where isolating the effect of any single variable becomes challenging. The weak statistical correlation observed in this study does not indicate that sea level rise is unimportant for shoreline change. Rather, it reflects the reality that shoreline position results from complex interplay among tidal action, sediment supply, human activities, river damming, coastal infrastructure, and sea level rise (Cooper and Pilkey, 2004; Ranasinghe et al., 2011; Toimil et al., 2020), all of which can themselves be affected by climate change.

This synergistic relationship, where multiple drivers interact non-linearly, has been documented in coastal systems globally (Mentaschi et al., 2018; Vousdoukas et al., 2020). The observed quasi-linear pattern in the correlation analysis likely reflects this complexity, where the impact of sea level rise is modulated by additional variables operating at multiple temporal and spatial scales. This exploratory analysis was not designed to isolate the causal contribution of sea-level rise to shoreline change, but rather to contextualize observed shoreline behavior within broader climate-driven trends alongside dominant local controls such as coastal engineering structures and sediment dynamics. The absence of a significant relationship suggests that at sites with major engineering interventions, the signal of gradual sea-level rise may be masked or overridden by the immediate effects of structural controls on sediment transport and wave dynamics (Barnard et al., 2019).

Management Implications for Ghana's Eastern Coast

The contrasting outcomes between protected and unprotected portions within the Dzita study area, combined with downdrift impacts documented at Kedzi and Hlorve by Adu-Gyamfi et al. (2020), highlight a critical challenge in coastal management. Structural interventions that successfully protect one area may simultaneously increase vulnerability elsewhere. These findings echo global concerns about hard structure stabilization. A comprehensive review of coastal erosion protection strategies found that while hard engineering structures like seawalls, breakwaters, and groynes remain the dominant approach, representing more than 70% of protected shorelines in Europe, they often have unintended consequences of moving erosion problems to adjacent coastal segments (Angnuureng et al., 2025).

Modern coastal management increasingly recognizes that while structural defences can be effective locally, integrated approaches are necessary for sustainable long-term solutions. The findings emphasize the importance of adaptive, data-driven coastal management strategies that account for both the protective benefits of infrastructure and potential unintended consequences. Contemporary approaches have shifted from initial reliance on hard structures toward management strategies such as sand-bypassing and managed retreat, with emerging trends toward hybrid systems combining both hard structures and management strategies (Saengsupavanich et al., 2024). Future coastal planning should consider these integrated approaches that balance structural protection with comprehensive sediment management and long-term monitoring to track both intended and unintended outcomes of interventions.

Conclusion

This study of Ghana's Dzita coast (2001-2023) found that coastal defence structures successfully reversed erosion trends at the protected site, shifting from severe erosion (-4.0 m/year) to net accretion (+1.7 m/year). However, this local success came at a regional cost: the defence system generated severe downdrift erosion at nearby communities like Kedzi and Hlorve (reaching -8 m/year), illustrating how structural interventions can redistribute rather than eliminate erosion. Statistical analysis revealed a weak correlation between shoreline change and global mean sea level rise (Spearman's p-value = 0.5774), underscoring that shoreline dynamics result from complex interactions among coastal structures, sediment transport, tidal processes, human activities, and climate-driven changes. This complexity demands adaptive management approaches that account for multiple interacting factors rather than isolated responses to sea level rise alone. The findings emphasize that effective adaptation to rising seas requires moving beyond reactive, site-specific structural solutions toward comprehensive regional strategies that integrate structural protection with sediment management and nature-based solutions. Coastal managers should establish continuous satellite-based monitoring programs to track both protective benefits and unintended consequences, incorporate regional sediment transport dynamics into planning to anticipate downdrift impacts, and utilize local sea level data rather than global averages for adaptation planning. Successfully adapting to rising seas in the context of climate change

requires acknowledging that coastal protection influences adjacent areas through altered sediment dynamics. The systematic monitoring framework demonstrated in this study provides a foundation for integrated approaches that balance immediate protection needs with long-term sustainability and work with natural coastal processes rather than attempting to rigidly control them.

Supplementary Data

The following supplementary data are available with the online version of this study:

Supplementary Data S1. Complete computational workflow (Jupyter notebook). This file contains the full Python code, processing parameters, and step-by-step methodology for shoreline extraction, MNDWI calculation, tidal modeling, composite generation, and rate of change calculations as adapted from Digital Earth Africa's coastline products.

Supplementary Data S2. Shoreline change rates for the Dzita coast (2001-2023). This dataset contains annual shoreline change distances (in meters) for all reference points spaced at 20-meter intervals along the coastline, relative to the 2023 baseline. Data includes both pre-defence (2001-2014) and post-defence (2014-2023) periods. (Both GeoJSON and Spreadsheet file types are available).

Supplementary Data S3. Extracted annual shoreline positions for the Dzita coast (2001-2023). This dataset contains the GeoJSON files of shoreline positions extracted from Landsat 7 imagery using MNDWI and sub-pixel contour mapping methods for each year of the study period.

Supplementary Data S4. Global mean sea level data (1993-2024). This dataset contains annual mean global sea level measurements from NASA's Sea Level Change Program (Beckley et al., 2017), accounting for global isostatic adjustment with annual and semi-annual signals removed.

References

Adu-Gyamfi, B., Shaw, R., and Yan, W. (2020). Assessment of housing exposure to accelerated coastal erosion in Keta Municipality of Ghana. *International Journal of Disaster Risk Reduction*, 44:101450. https://doi.org/10.1016/J.IJDRR.2019.101450.

Akpati, B. N. (1978). Geologic structure and evolution of the Keta basin, Ghana, West Africa. *GSA Bulletin*, 89(1):124–132. https://doi.org/10.1130/0016-7606(1978)89<124:GSAEOT>2.0.CO;2.

Angnuureng, B. D., Adade, R., Chuku, E. O., Dzantor, S., Brempong, E. K., and Mattah, P. A. D. (2023). Effects of coastal protection structures in controlling erosion and livelihoods. *Heliyon*, 9(10):e20633. https://doi.org/10.1016/j.heliyon.2023.e20633.

Angnuureng, D. B., Charuka, B., Almar, R., Dada, O. A., Asumadu, R., Agboli, N. A., and Ofosu, G. T. (2025). Challenges and lessons learned from global coastal erosion protection strategies. *iScience*, 28(4):112055. https://doi.org/10.1016/j.isci.2025.112055.

Appeaning Addo, K., Jayson-Quashigah, P. N., and Kufogbe, K. S. (2011). Quantitative Analysis of Shoreline Change Using Medium Resolution Satellite Imagery in Keta, Ghana. *Marine Science*, 1(1):1–9. https://doi.org/10.5923/j.ms.20110101.01.

Awadzi, T. W., Ahiabor, E., and Breuning-Madsen, H. (2008). The Soil-Land use System in a Sand Spit Area in the Semi-Arid Coastal Savanna Region of Ghana-Development, Sustainability and Threats. *West African Journal of Applied Ecology*, 13. https://www.ajol.info/index.php/wajae.

Balaji, R., Kumar, S. S., and Misra, A. (2017). Understanding the effects of seawall construction using a combination of analytical modelling and remote sensing techniques: Case study of Fansa, Gujarat, India. *The International Journal of Ocean and Climate Systems*, 8(3):153–160. https://doi.org/10.1177/1759313117712180.

Barnard, P. L., Erikson, L. H., Foxgrover, A. C., Hart, J. A. F., Limber, P., O'Neill, A. C., van Ormondt, M., Vitousek, S., Wood, N., Hayden, M. K., and Jones, J. M. (2019). Dynamic flood modeling essential to assess the coastal impacts of climate change. *Scientific Reports*, 9(1):4309. https://doi.org/10.1038/s41598-019-40742-z.

Beckley, B. D., Callahan, P. S., Hancock, D. W., Mitchum, G. T., and Ray, R. D. (2017). On the 'cal-mode' correction to TOPEX satellite altimetry and its effect on the global mean sea level time series. *Journal of Geophysical Research: Oceans*, 122. https://doi.org/10.1002/2017JC013090.

Bishop-Taylor, R., Nanson, R., Sagar, S., and Lymburner, L. (2021a). Digital Earth Australia Coastlines. Technical report, Geoscience Australia. https://doi.org/10.26186/116268.

Bishop-Taylor, R., Nanson, R., Sagar, S., and Lymburner, L. (2021b). Mapping Australia's dynamic coastline at mean sea level using three decades of Landsat imagery. *Remote Sensing of Environment*, 267:112734. https://doi.org/10.1016/j.rse.2021.112734.

Bishop-Taylor, R., Sagar, S., Lymburner, L., Alam, I., and Sixsmith, J. (2019). Sub-Pixel Waterline Extraction: Characterising Accuracy and Sensitivity to Indices and Spectra. *Remote Sensing*, 11(24):2984. https://doi.org/10.3390/rs11242984.

Boateng, I. (2009). Development of integrated shoreline management planning: A case study of Keta, Ghana. In *Proceedings of the Federation of International Surveyors Working Week 2009*, pages 3–8,

Eilat, Israel. https://www.fig.net/resources/proceedings/fig_proceedings/fig2009/papers/ts04e/ts04e_boateng_3577.pdf.

Boateng, I. (2012). An application of GIS and coastal geomorphology for large scale assessment of coastal erosion and management: a case study of Ghana. *Journal of Coastal Conservation*, 16(3):383–397. https://doi.org/10.1007/s11852-012-0209-0.

Carrere, L., Lyard, F., Cancet, M., Guillot, A., and Picot, N. (2016). FES2014, a new tidal model – Validation results and perspectives for improvements. In *ESA Living Planet Conference*, Prague.

Cazenave, A. and Le Cozannet, G. (2014). Sea level rise and its coastal impacts. *Earth's Future*, 2(2):15–34. https://doi.org/10.1002/2013EF000188.

Cooper, J. A. G. and Pilkey, O. H. (2004). Sea-level rise and shoreline retreat: time to abandon the Bruun Rule. *Global and Planetary Change*, 43(3):157–171. https://doi.org/10.1016/j.gloplacha.2004.07.001.

Danquah, J. A., Attippoe, J. A., and Ankrah, J. S. (2014). Assessment of residential satisfaction in the resettlement towns of the Keta basin in Ghana. *International Journal Civil Engineering, Construction and Estate Management*, 2(3):26–45.

Hoyer, S. and Hamman, J. (2017). xarray: ND labeled arrays and datasets in Python. *Journal of Open Research Software*, 5(1):10. https://doi.org/10.5334/jors.148.

Ile, I. U., Garr, E. Q., and Ukpere, W. I. (2014). Monitoring infrastructure policy reforms and rural poverty reduction in Ghana: the case of Keta Sea Defence Project. *Mediterranean Journal of Social Sciences*, 5(3):633–642. https://doi.org/10.5901/mjss.2014.v5n3p633.

IPCC (2023). *Climate Change 2021 – The Physical Science Basis: Working Group I Contribution to the Sixth Assessment Report of the Intergovernmental Panel on Climate Change*. Cambridge University Press. https://doi.org/10.1017/9781009157896.

Jayson-Quashigah, P. N., Appeaning Addo, K., and Kufogbe, S. K. (2013). Shoreline monitoring using medium resolution satellite imagery, a case study of the eastern coast of Ghana. In *Journal of Coastal Research*, volume 65, pages 511–516. Coastal Education & Research Foundation. https://doi.org/10.2112/SI65-087.1.

Krause, C., Dunn, B., Bishop-Taylor, R., Adams, C., Burton, C., Alger, M., Chua, S., Phillips, C., Newey, V., and Kouzoubov, K. (2021). Digital Earth Australia notebooks and tools repository. Geoscience Australia. https://github.com/GeoscienceAustralia/dea-notebooks.

Le Cozannet, G., Rohmer, J., Cazenave, A., Idier, D., van de Wal, R., de Winter, R., Pedreros, R., Balouin, Y., Vinchon, C., and Oliveros, C. (2015). Evaluating uncertainties of future marine flooding occurrence as sea-level rises. *Environmental Modelling & Software*, 73:44–56. https://doi.org/10.1016/j.envsoft.2015.07.021.

Ly, C. K. (1980). The role of the Akosombo Dam on the Volta river in causing coastal erosion in central and eastern Ghana (West Africa). *Marine Geology*, 37(3–4):323–332. https://doi.org/10.1016/0025-3227(80)90108-5.

Masek, J. G., Vermote, E. F., Saleous, N. E., Wolfe, R., Hall, F. G., Huemmrich, K. F., Gao, F., Kutler, J., and Lim, T. K. (2006). A Landsat surface reflectance dataset for North America, 1990-2000. *IEEE Geoscience and Remote Sensing Letters*, 3(1):68–72. https://doi.org/10.1109/LGRS.2005.857030.

Mentaschi, L., Vousdoukas, M. I., Pekel, J. F., Voukouvalas, E., and Feyen, L. (2018). Global long-term observations of coastal erosion and accretion. *Scientific Reports*, 8(1):12876. https://doi.org/10.1038/s41598-018-30904-w.

Nassar, K., Mahmod, W. E., Fath, H., Masria, A., Nadaoka, K., and Negm, A. (2018). Shoreline change detection using DSAS technique: Case of North Sinai coast, Egypt. *Marine Georesources & Geotechnology*, 37(1):81–95. https://doi.org/10.1080/1064119X.2018.1448912.

Oteng-Ababio, M. and Owusu, K. (2011). The vulnerable state of the Ghana coast: The case of Faana-Bortianor. *Jàmbá: Journal of Disaster Risk Studies*, 3(2):429–442. https://doi.org/10.4102/jamba.v3i2.39.

Pang, T., Wang, X., Nawaz, R. A., Keefe, G., and Adekanmbi, T. (2023). Coastal erosion and climate change: A review on coastal-change process and modeling. *Ambio*, 52(12):2034–2052. https://doi.org/10.1007/s13280-023-01901-9.

Ranasinghe, R., Callaghan, D., and Stive, M. J. F. (2011). Estimating coastal recession due to sea level rise: beyond the Bruun rule. *Climatic Change*, 110(3):561–574. https://doi.org/10.1007/s10584-011-0107-8.

Rangel-Buitrago, N., Williams, A. T., and Anfuso, G. (2018). Hard protection structures as a principal coastal erosion management strategy along the Caribbean coast of Colombia. A chronicle of pitfalls. *Ocean & Coastal Management*, 156:58–75. https://doi.org/10.1016/j.ocecoaman.2017.04.006.

Saengsupavanich, C., Rif'atin, H. Q., Magdalena, I., and Ariffin, E. H. (2024). A systematic review of jetty-induced downdrift coastal erosion management. *Regional Studies in Marine Science*, 74:103523. https://doi.org/10.1016/j.rsma.2024.103523.

Toimil, A., Camus, P., Losada, I. J., Le Cozannet, G., Nicholls, R. J., Idier, D., and Maspataud, A. (2020). Climate change-driven coastal erosion modelling in temperate sandy beaches: Methods and uncertainty treatment. *Earth-Science Reviews*, 202:103110. https://doi.org/10.1016/j.earscirev.2020.103110.

USGS (2020). Landsat Collection 2. U.S. Geological Survey. https://www.usgs.gov/landsat-missions/landsat-collection-2.

Vousdoukas, M. I., Ranasinghe, R., Mentaschi, L., Plomaritis, T. A., Athanasiou, P., Luijendijk, A., and Feyen, L. (2020). Sandy coastlines under threat of erosion. *Nature Climate Change*, 10(3):260–263. https://doi.org/10.1038/s41558-020-0697-0.

World Meteorological Organization (2020). The Global Climate 2011-2020: A Decade of Accelerating Climate Change. World Meteorological Organization. https://library.wmo.int/records/item/68585-the-global-climate-2011-2020.

Xu, H. (2006). Modification of normalised difference water index (NDWI) to enhance open water features in remotely sensed imagery. *International Journal of Remote Sensing*, 27(14):3025–3033. https://doi.org/10.1080/01431160600589179.